A pair of integrated optoelectronic transceiving chips for optical interconnects

Kai Liu (刘凯)*, Huize Fan (范惠泽), Yongqing Huang (黄永清), Xiaofeng Duan (段晓峰),
Qi Wang (王琦), Xiaomin Ren (任晓敏), Qi Wei (位祺), and Shiwei Cai (蔡世伟)

State Key Laboratory of Information Photonics and Optical Communications, Beijing University of Posts and Telecommunications, Beijing 100876, China

*Corresponding author: kliu@bupt.edu.cn

Received July 10, 2018; accepted July 19, 2018; posted online August 31, 2018

In this Letter, a pair of integrated optoelectronic transceiving chips is proposed. They are constructed by integrating a vertical cavity surface emitting laser unit above a positive-intrinsic-negative photodetector unit. One of the transceiving chips emits light at the wavelength of 848.1 nm with a threshold current of 0.8 mA and a slope efficiency of 0.81 W/A. It receives light between 801 and 814 nm with a quantum efficiency of higher than 70%. On its counterpart, the other one of the transceiving chips emits light at the wavelength of 805.3 nm with a threshold current of 1.1 mA and a slope efficiency of 0.86 W/A. It receives light between 838 and 855 nm with a quantum efficiency of higher than 70%. The proposed pair of integrated optoelectronic transceiving chips can work full-duplex with each other, and they can be applied to single fiber bidirectional optical interconnects.

OCIS codes: 130.3120, 130.0250, 250.7260, 230.5160.

doi: 10.3788/COL201816.091301.

Accompanying the rapid developing demands for more and more information interconnect bandwidths, which are generated from the applications of ultra-wideband communications in the data center, a 5G wireless system, cloud computing, supercomputer fields, etc., the interconnect technology tends to utilize optical links to overcome the drawbacks of the electric links, like high power consumption, channel interference, complicated channel electrical isolation, etc. The optoelectronic devices, like a vertical cavity surface emitting laser (VCSEL)[1–4], a light emitting diode (LED)[5], a uni-traveling-carrier (UTC) photodetector (PD)[6,7], a positive-intrinsic-negative (PIN) PD[8], and a modulator[9–11], are important devices here for transferring information between the electrical signals and the optical signals. Some attempts to integrate the optical signal's transmitting and receiving functions from and to electrical signals into only one optoelectronic chip have been made for further increasing their performances[12,13]. Moreover, sometimes the optics structure and semiconductor diode are integrated with them too[14,15]. With these integration schemes, an on chip three-dimensional optical interconnection channel has been realized[16], and an integration platform has also been proposed[17]. In this Letter, a new integration scheme for realizing the optical signal's transmitting and receiving functions, named transceiving functions here, simultaneously with only one optoelectronic chip was proposed. It is constructed by integrating a VCSEL on top of a PIN-PD. With careful optical structure design, the VCSEL and the PIN-PD will emit and receive light at different wavelengths. The two units are also electrically isolated from each other by inserting electrical insulating structures between them. Then, to construct the optical interconnects with the proposed pair of transceiving chips,

at one end, the VCSEL will emit light at the wavelength around 850 nm and receive light at the wavelength around 800 nm; while at the other end, the VCSEL will emit light at the wavelength around 800 nm and receive light at the wavelength around 850 nm. Since the VCSEL and the PIN-PD are integrated vertically and coaxially, it will further simplify the chip's future coupling scheme to a multimode fiber, while being used for the application of bidirectional full-duplex optical interconnects in a single fiber and lower the packaging cost at the same time. In the following part of the Letter, we will present the optical structure design and device performance simulations of the pair of the integrated transceiving chips.

The structure of the proposed integrated optoelectronic transceiving chip is shown in Fig. 1. It is composed of a VCSEL unit at the top and a PIN-PD unit at the bottom.
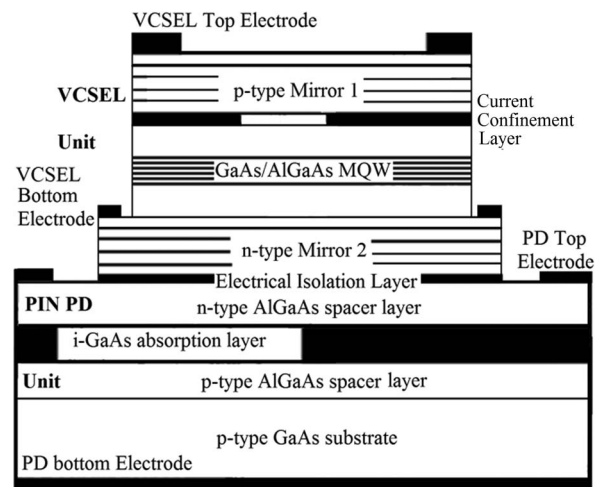
Fig. 1. Transceiving chip's structure.

To allow such a chip to transmit and receive the optical signal simultaneously, electrical performance isolation and optical function decoupling between its two composing units must be accomplished. In the chip's structural design, the electrical performance isolation is accomplished by inserting an insulating layer between its two composing units. It can be realized by growing an $Al_{0.98}Ga_{0.02}As$ layer during the chip structure's epitaxy growth and then transferring this $Al_{0.98}Ga_{0.02}As$ layer into an Al_2O_3 electrical insulating layer with wet oxidation during the chip process. The optical function decoupling is accomplished by the wavelength division multiplexing scheme. Since full-duplex working is required for the proposed integrated optoelectronic transceiving chip, its particular working optical spectra will be set. The transmitting light wavelength is set to be around 850 nm, and the receiving light wavelength is set to be around 800 nm at one end. Correspondingly, the transmitting light wavelength is set to be around 800 nm, and the receiving light wavelength is set to be around 850 nm at the other end of the optical interconnects channel.

For the proposed transceiving chip's structure, the main problem that should be solved is the structure design of mirrors 1 and 2. They should have high reflectivity at the transmitting light wavelength and low reflectivity at the receiving light wavelength to make the VCSEL unit work properly and allow the PIN-PD unit to work with high absorption quantum efficiency (AQE). Then, a distributed Bragg reflector (DBR) in the cavity structure is proposed to accomplish such a purpose. The cavity resonance wavelength is set at the receiving wavelength. The DBR's central wavelength is set at the transmitting wavelength. So, one of the transceiving chips' mirror cavity resonance wavelength is set at 805 nm, its DBR's central wavelength is set at 850 nm, and they are composed of alternately grown $Al_{0.15}Ga_{0.85}As/Al_{0.9}Ga_{0.1}As$ layers. The chip's VCSEL active region is composed of three pairs of $Al_{0.3}Ga_{0.7}As/GaAs$ quantum wells and emits light at wavelengths around 850 nm. The other one of the transceiving chips' mirror cavity wavelength is set at 850 nm, its DBR's central wavelength is set at 805 nm, and they are also composed of alternately grown $Al_{0.15}Ga_{0.85}As/Al_{0.9}Ga_{0.1}As$ layers. The chip's VCSEL active region is composed of three pairs of $Al_{0.3}Ga_{0.7}As/Al_{0.06}Ga_{0.94}As$ quantum wells and emits light at wavelengths around 805 nm. Both of the transceiving chips' PIN-PD units have a 2.1 μm thick un-doped GaAs absorption layer sandwiched between a p-doped $Al_{0.2}Ga_{0.8}As$ layer and an n-doped $Al_{0.2}Ga_{0.8}As$ layer. The obtained transceiving chips' reflection spectra are shown in Fig. 2. Next, the device performance simulations will be done.

In the simulation, the effective frequency method[18] and self-consistent two-dimensional model[19] were adopted. The material parameters were taken from Ref. [19]. For the device's structure size, the VCSEL unit's size is set with a radius of 13 μm, the PIN-PD unit's size is set with a radius of 25 μm, the current aperture size of the VCSEL
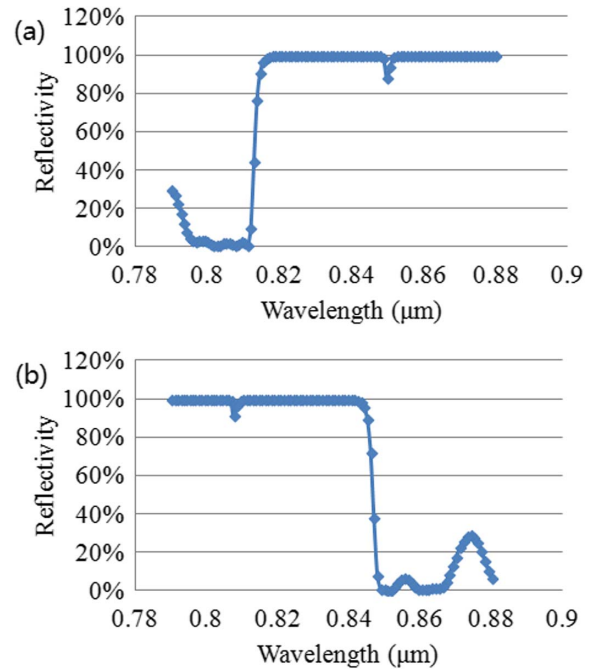
Fig. 2. Transceiving chip's reflection spectra: (a) the chip that transmits light at a wavelength around 850 nm and receives light at a wavelength around 805 nm; (b) the chip that transmits light at a wavelength around 805 nm and receives light at a wavelength around 850 nm.

unit is set with a diameter of 6 μm in the center of the current confinement layer, and the electrodes are set as shown in Fig. 1. The VCSEL's bottom electrode and the PIN-PD's top electrode are set to be connected to the ground.

First, the VCSEL unit's static performance is simulated. It is forward biased from 0 to 1.9 V, corresponding to a forward biasing current from 0 to 11.3 mA for the VCSEL emitting at a wavelength around 850 nm and a forward biasing current from 0 to 9.95 mA for the VCSEL emitting at a wavelength around 805 nm. The simulation results are shown in Fig. 3. It can be drawn from Fig. 3(a) that a threshold current of 0.8 mA and a slope efficiency of 0.81 W/A are obtained for the VCSEL unit emitting at a wavelength around 850 nm. The simulated lasing wavelength is located at 848.1 nm, and the obtained maximal output light power is 8.86 mW. Figure 3(b) shows that a threshold current of 1.1 mA and a slope efficiency of 0.86 W/A are obtained for the VCSEL unit emitting at a wavelength around 805 nm. The simulated lasing wavelength is located at 805.3 nm, and the obtained maximal output light power is 7.56 mW. Both VCSEL units are working with a fundamental lateral mode for obtaining high coupling efficiency to multimode fibers.

To evaluate the influence of the VCSEL unit's performance on the PIN-PD unit's performance, the photoresponse currents of PIN-PD unit at the different VCSEL unit's output light powers are shown in Fig. 4. Here, both of the transceiving chips' PIN-PD units are biased at −5.0 V. The simulated results show that within the
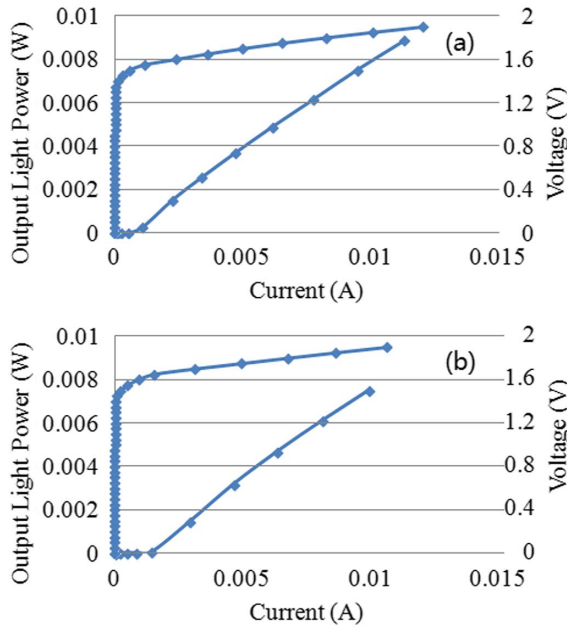
Fig. 3. VCSEL unit's static performance: (a) the chip that transmits light at a wavelength around 850 nm, where the simulated lasing wavelength is at 848.1 nm; (b) the chip that transmits light at a wavelength around 805 nm, where the simulated lasing wavelength is at 805.3 nm.
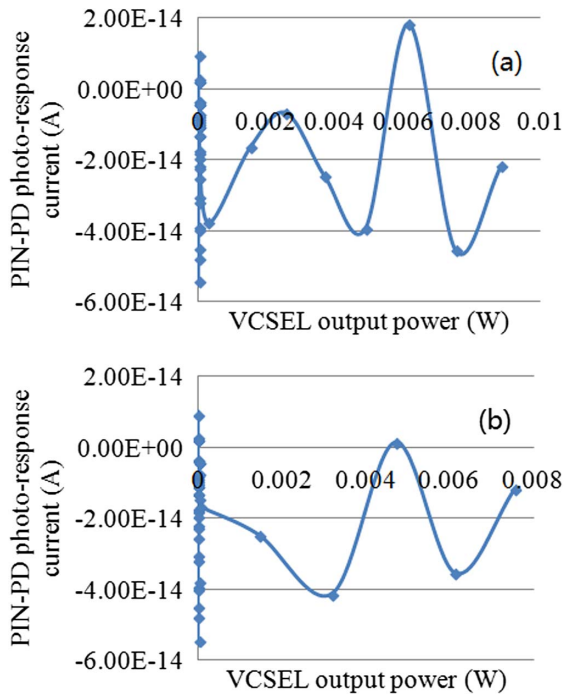
Fig. 4. PIN-PD unit's photo-response performance upon the VCSEL unit's output light power: (a) the chip that transmits light at a wavelength of 848.1 nm; (b) the chip that transmits light at a wavelength of 805.3 nm.

simulated VCSEL unit's output light power range, the PIN-PD unit's photo-response currents are randomly distributed between -5×10^{-14} A and 2×10^{-14} A. It means that almost no output light power from the VCSEL unit

will get into the PIN-PD unit. Such results are due to the optimization of the integrated transceiving chip's optical structure design. At the VCSEL unit's lasing wavelength (848.1 or 805.3 nm), mirror 2 is designed to have a higher reflectivity than mirror 1. It guarantees that the VCSEL unit's lasing light power will emit from mirror 1 and it especially makes sure that the backlight of the VCSEL unit will be terminated within mirror 2. The simulation results prove that here. Therefore, for the integrated transceiving chips, their VCSEL units' optical performances will have little effect on their PIN-PD units' photo-response performances.

Thereafter, the spectral photo-response performances of the integrated transceiving chips are simulated. Here, their VCSEL units are biased at 1.9 V (above the threshold conditions), and their PIN-PD units are biased at -5 V. The input light intensity is set to be 10 W/cm^2, and its wavelength is set to change from 0.79 to 0.88 μm. The obtained AQE spectra of the integrated transceiving chips are shown in Fig. 5. Figure 5(a) shows that the transceiving chip that transmits light at a wavelength of 848.1 nm obtains a photo-response spectral range that changes from 801 to 814 nm with an AQE of higher than 70% for its PIN-PD unit. At the wavelength of 805.3 nm, its PIN-PD unit's AQE is 85%. At the same time, the AQE of its VCSEL unit is almost 0 (lower than 3‰). On its counterpart, as shown in Fig. 5(b), the transceiving chip that transmits light at a wavelength of 805.3 nm obtains a photo-response spectral range that changes from 838 to 855 nm with an AQE of higher than 70% for its PIN-PD unit. At the wavelength of 848.1 nm, its PIN-PD unit's AQE is 76.1%. At the same time, the AQE of its VCSEL unit is almost 0 (lower than 0.05%). Moreover, the transceiving chips' photo-response
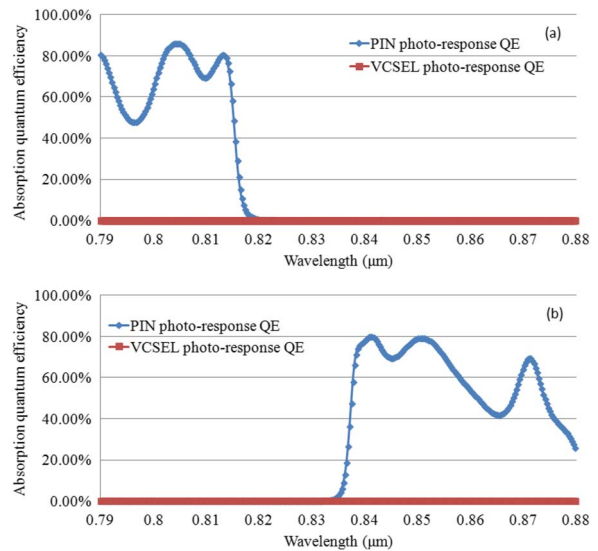
Fig. 5. Spectral photo-response performances of the integrated transceiving chips: (a) the chip that transmits light at a wavelength of 848.1 nm and receives light at a wavelength around 805 nm; (b) the chip that transmits light at a wavelength of 805.3 nm and receives light at a wavelength around 850 nm.
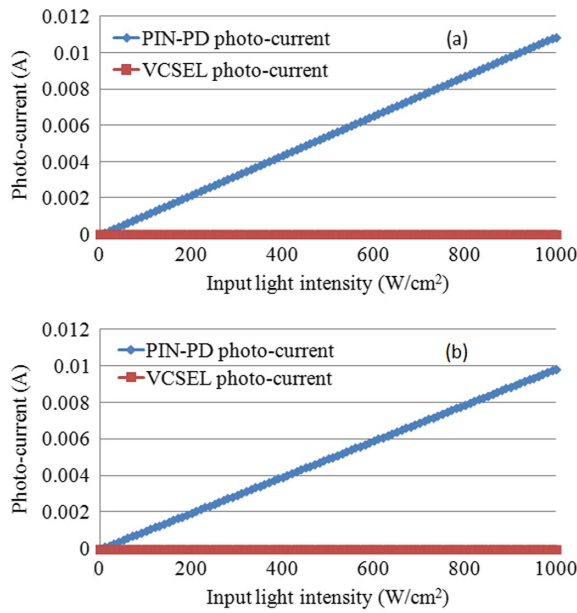
Fig. 6. Photo-response performances of the integrated transceiving chips with the input light intensity changing from 0 to 1000 W/cm^2: (a) the chip that receives light at a wavelength of 805.3 nm; (b) the chip that receives light at a wavelength of 848.1 nm.

Fig. 7. Electrical isolation performances of the integrated transceiving chips represented by the analysis of the S21 parameter: (a) the AC signal applied on the VCSEL electrode; (b) the AC signal applied on the PIN-PD electrode.

performances at wavelengths of 848.1 or 805.3 nm with input light intensity changing from 0 to 1000 W/cm^2 are shown in Fig. 6.

Furthermore, to evaluate the electrical isolation effect between the integrated chip's two units under dynamic conditions, the small AC modulating signal will be set on either the VCSEL unit's electrode or the PIN-PD unit's electrode separately. The electrical response from the other electrode should be as small as possible for a better electrical isolation performance. Thus, we can take the proposed integrated chip as a two-port network. The VCSEL unit's electrodes form one port of the network and the PIN-PD unit's electrodes form the other port. The electrical isolation effect between the two units can be represented by the S21 parameter of the two-port network. The analysis is made under modulation frequency changing from 1 MHz to 100 GHz. In the analysis, the VCSEL unit is forward biased at 1.9 V, the PIN-PD unit is biased at −5 V, and the small AC signal's amplitude is set to be 0.02 V. First, the AC signal is applied to the VCSEL unit's top electrode. The obtained S21 frequency spectrum is shown in Fig. 7(a). It shows that up to 22.6 GHz the S21 parameter's value is smaller than −50 dB for both transceiving chips. Secondly, the AC signal is applied to the PIN-PD unit's bottom electrode. The obtained S21 parameter frequency spectrum is shown in Fig. 7(b). It shows that up to 100 GHz the S21 parameter's value is smaller than −50 dB. So, it can be concluded that the integrated transceiving chip's two units are electrically isolated for frequencies up to 22.6 GHz.

As mentioned above, a pair of integrated transceiving chips is proposed. It is constructed by integrating a

VCSEL unit above a PIN-PD unit. Analysis shows that one of the transceiving chips emits light at a wavelength of 848.1 nm with a threshold current of 0.8 mA and a slope efficiency of 0.81 W/A. It receives light between 801 and 814 nm with a quantum efficiency of higher than 70%. On its counterpart, the other one of the transceiving chips emits light at a wavelength of 805.3 nm with a threshold current of 1.1 mA and a slope efficiency of 0.86 W/A. It receives light between 838 and 855 nm with a quantum efficiency of higher than 70%. Moreover, the two composing units of the proposed transceiving chip can work electrically isolated and optically decoupled from each other. The proposed integrated transceiving chips can work at full-duplex, and they can be applied for further performance improvement of the optical interconnects system.

References
1. P.-K. Shen, C.-T. Chen, and C.-H. Chang, IEEE Photon. J. **6**, 2500310 (2014).
2. H. Qiu, Z. Wu, T. Deng, Y. He, and G. Xia, Chin. Opt. Lett. **14**, 021401 (2016).
3. Y. Feng, L. Hou, Y. Hao, C. Yan, Y. Zhao, Y. Wang, and J. Zhong, Chin. Opt. Lett. **8**, 773 (2010).
4. H.-Y. Kao, Y.-C. Chi, C.-T. Tsai, S.-F. Leong, C.-Y. Peng, H.-Y. Wang, J. J. Huang, J.-J. Jou, T.-T. Shih, H.-C. Kuo, W.-H. Cheng, C.-H. Wu, and G.-R. Lin, Photon. Res. **5**, 507 (2017).

5. M. Riester and R. Houbertz, in *Proceedings of World Telecommunications Congress* (2014), p. 1.

6. F.-M. Kuo, T.-C. Hsu, and J.-W. Shi, in *OFC* (2009), p. 1.

7. T. Shi, B. Xiong, C. Sun, and Y. Luo, Chin. Opt. Lett. **9**, 082302 (2011).

8. H. Nasu, T. Kise, K. Nagashima, and N. Nishimura, in *The European Conference on Optical Communication (ECOC)* (2014), paper Tu.4.5.2.

9. S. Shimizu, X. Gu, and T. Shimada, in *2nd IEEE CPMT Symposium Japan* (2012), p. 1.

10. X. Li, F. Yang, F. Zhong, Q. Deng, M. Jurgen, and Z. Zhou, Photon. Res. **5**, 134 (2017).

11. B.-M. Yu, M. Shin, M.-H. Kim, L. Zimmermann, and W.-Y. Choi, Chin. Opt. Lett. **15**, 071301 (2017).

12. G. Hasnain, K. Tai, Y. H. Wang, J. D. Wynn, K. D. Choquette, B. E. Weir, N. K. Durra, and A. Y. Cho, Electron. Lett. **27**, 1630 (1991).

13. G. G. Ortiz, C. P. Hains, J. Cheng, H. Q. Hou, and J. C. Zolper, Electron. Lett. **32**, 1205 (1996).

14. F. E. Doany, C. L. Schow, C. W. Baks, and D. M. Kuchta, IEEE Trans. Adv. Packag. **32**, 345 (2009).

15. J. Mi, H. Yu, H. Wang, and S. Tan, IEEE Photon. Technol. Lett. **27**, 169 (2015).

16. P.-K. Shen, C.-T. Chen, S.-L. Li, C.-H. Chang, S.-H. Lin, C.-C. Chang, H.-C. Lan, and M.-L. Wu, in *18th Microoptics Conference (MOC'13)* (2013), p. 1.

17. E. J. Norberg, B. R. Koch, J. E. Roth, A. Ramaswamy, R. S. Guzzon, D. K. Sparacin, and G. A. Fish, in *IEEE Photonics Conferrence (IPC)* (2015), p. 351.

18. H. Wenzel and H.-J. Wunsche, IEEE J. Quantum Electron. **33**, 1156 (1997).

19. Z.-M. Li, K. M. Dzurko, A. Dellge, and S. P. McAlister, IEEE J. Quantum Electron. **28**, 1209 (1992).